uge for subtidal populations, allowing the whelk to expand on the removal of predation pressure. In situ caging experiments indicate that *Burnupena* spp. cannot attack healthy mussels although they feed readily on damaged or dying mussels. Mussels in turn are filter-feeders that derive their food from the water column. The two populations are thus incapable of eliminating their own food source and can maintain high densities in the absence of their chief predator, the rock lobster. Thus *Burnupena* spp. can reverse their normal role as prey for rock lobsters and exclude the latter from Marcus Island (Fig. 4).

REFERENCES AND NOTES

1. W. P. Sousa, S. C. Schroeter, S. D. Gaines, *Oecologia* **48**, 297 (1981); J. H. Connell and M. J. Keough, in *Natural Disturbance: The Patch Dynamics Perspective*, S. T. A. Pickett and P. S. White, Eds. (Academic Press, New York, 1985), pp. 125–151; P. K. Dayton, *Ecol. Monogr.* **55**, 447 (1985); K. Hiscock, in *The Ecology of Rocky Coasts*, P. G. Moore and R. Seed, Eds. (Hodder & Stoughton, London, 1985), pp. 290–328.
2. P. A. Luckens, *N.Z. J. Mar. Fresh. Res.* **9** (no. 3), 379 (1975); S. D. Garrity and S. C. Levings, *Mar. Biol.* 72, 319 (1983); M. J. Tegner and A. Levin, *J. Exp. Mar. Biol. Ecol.* **73**, 1 (1983); P. K. Dayton *et al.*, *Ecol. Monogr.* **54**, 253 (1984); P. G. Fairweather, A. J. Underwood, M. J. Moran, *Mar. Ecol. Prog. Ser.* **17**, 143 (1984); A. J. Penny and C. L. Griffiths, *J. Exp. Mar. Biol. Ecol.* **75**, 19 (1984); R. N. Hughes, in *The Ecology of Rocky Coasts*, P. G. Moore and R. Seed, Eds. (Hodder & Stoughton, London, 1985), pp. 223–233; C. W. Thayer, *Science* **228**, 1526 (1985).
3. K. H. Mann and P. A. Breen, *J. Fish. Res. Board Can.* **29**, 603 (1972); C. A. Simenstad, J. A. Estes, K. W. Kenyon, *Science* **200**, 403 (1978); R. T. Paine, *Ecology* **49**, 667 (1980).
4. R. C. Lewontin, *Brookhaven Symp. Biol.* **22**, 13 (1969); J. P. Sutherland, *Am. Nat.* **108**, 859 (1974).
5. J. H. Connell and W. P. Sousa, *Am. Nat.* **121**, 789 (1983); *ibid.* **125**, 612 (1985).
6. A. Barkai, thesis, University of Cape Town, Cape Town, South Africa (1987); ——— and G. M. Branch, *S. Afr. J. Mar. Sci.*, in press.
7. *t* test; $P < 0.001$ (54 mm ± 6.9 mm at Malgas Island and 36 mm ± 7.5 mm at Marcus Island).
8. Chi-square test; $P < 0.001$ in both cases.
9. One-way ANOVA; $P < 0.05$.
10. It was not possible to perform a comparable experiment with *B. limbosa*, as the damaged shells of this species are difficult to distinguish from cleaned *B. papyracea* shells.
11. Significantly lower than 33% of the total; chi-square test; $P < 0.001$.
12. Chi-square test; $P > 0.05$.
13. Mean increased significantly, *t* test; $P < 0.001$.
14. S. M. Al-Ogily and E. W. Knight-Jones, *Nature* **265**, 728 (1977); J. S. Carle and C. Christophersen, *J. Am. Chem. Soc.* **102**, 5107 (1980).
15. These consisted of 2 × 0.5 ton, 1-m^3 concrete blocks with 200-cm diameter passages running through them.
16. G. G. Newman and D. E. Pollock, *S. Afr. J. Sci.* **69**, 27 (1973); N. D. Christie and A. Moldan, *Mar. Pollut. Bull.* **8** (no. 2), 41 (1977).
17. R. T. Paine, *Oecologia* **15**, 93 (1974).
18. N. G. Hairston, F. E. Smith, L. B. Slobodkin, *Am. Nat.* **94**, 421 (1960); G. Caughley, *Ecology* **51**, 53 (1970); D. R. Klein, in *Animal Populations in Relation to Their Food Resources*, A. Watson, Ed. (Blackwell, Oxford, 1970), pp. 25–46.
19. We thank G. M. Branch, R. Barkai, members of the Sea Fisheries Research Institute at Saldanha Bay, the Research Diving Unit of the University of Cape Town, and many friends and colleagues in the Zoology Department at the University of Cape Town, for assistance with this research.

2 March 1988; accepted 6 July 1988

Catastrophic Landslide Deposits in the Karakoram Himalaya

KENNETH HEWITT

In July 1986, three catastrophic landslides deposited about 20 × 10^6 cubic meters of debris on Bualtar Glacier in the Karakoram Himalaya. A sudden acceleration and superficial breakup of the glacier provided an opportunity to examine the fresh deposits in depth. Beneath a surface layer of large boulders, finer materials, mainly sand and silt, made up half of the total volume. The fine materials were formed during the rock avalanche from mostly intact, massive rock of the source zone. Velocity estimates suggest that this disaggregation occurred in less than 2 minutes. Coarse materials remained in bands of uniform lithology, but the fine materials had diffused throughout the landslides. A small amount of carbonate appears to have been calcined by frictional heating, presumably at the base of the initial sliding masses. These observations are relevant to understanding the mechanisms of catastrophic landslides. Other nearby rock avalanche deposits indicate that landslides are an important geomorphic process in the area and that they pose a continuing risk to human activity.

THREE LARGE ROCK AVALANCHES descended to the surface of Bualtar Glacier in the central Karakoram Himalaya between 29 and 31 July 1986 (*1*). Approximately 20 × 10^6 m^3 of debris were deposited on the ice (Fig. 1). The maximum descent of the first, most extensive landslide, Bualtar I, was 1490 m. It traveled 4.8 km horizontally and covered 4.1 km^2 of the ice (Fig. 2). Its debris remained fairly dry throughout. However, the second and third rock avalanches became saturated in the run-out zone, presumably from melted ice. Five months after the landslides, the glacier suddenly accelerated from measured flow rates of 0.6 to 0.8 m day^{-1} to more than 7.0 m day^{-1} in and below the debris-covered area. This surge carried the deposits 2 km down-valley between January and August 1987 (*2*) and broke the deposits up, which provided a rare opportunity to examine fresh rock avalanche deposits in complete sections.

The landslide sequence began midafternoon on 25 July with a large rockfall from just below where the three rock avalanches would originate. The timing of the rock avalanches is deduced from the occurrence of three major dustfall episodes, which were reported up to 25 km away, in the evening and night of 29, 30, and 31 July. The landslides were not observed in progress, nor found until a rainstorm cleared the air of their dust.

The source rocks, assigned to the Chalt Series of Cretaceous to Eocene age, are mainly schist and marble (*3*). Bedding planes, which dip at 50° or more and are subparallel to the slope, were the main surfaces of rupture and initial sliding. The breakout zone is also defined by major near-vertical joints. The landslides occurred during the melting of a larger than normal winter snowpack and during a period of heavy rainstorms. The regulation of meltwater supply by diurnal freeze-thaw cycles seems to have been the trigger for a sequence of failures on successive days and late in each day (*4*).

The actual movement of rock avalanches is rarely observed; therefore, aspects of their geometry that may indicate transport mechanisms are of special interest (Table 1). The geometry of Bualtar I places it in Hsu's "more mobile" class (*5*). Its average speed of descent to the glacier was approximately 62 m s^{-1}, and it had a velocity over the ice of at least 44 m s^{-1}. Its probable maximum velocity at impact with the glacier was 124 m s^{-1} more than 440 km $hour^{-1}$. Hence, the entire landslide was deposited in less than 100 s (*6*). Rock avalanche researchers have focused on mechanisms that can cause such mobility through reduced friction in the run-out zone. Some workers also emphasize conditions of initial sliding that promote rapid acceleration. The Bualtar deposits have a bearing on both questions.

The debris was spread over the glacier in

Snow and Ice Hydrology Project, Wilfrid Laurier University, Waterloo, Ontario, Canada N2L 3C5.

huge sheets, 4 to 10 m thick (Fig. 3). Surface depositional forms included lobes, tongue-like run-out features and raised rims (7). Boulders, mainly 0.5 to 4.0 m in diameter, covered 90% of the surface. Dozens of boulders were greater than 20 m in diameter, and one was 44 m. Beneath this surface layer, some 40 to 60% of the material in most sections consisted of size fractions smaller than cobbles (<64 mm). Most matrix was silty-sand sized, with 15 to 35% fines (<0.075 mm), but with 5% or less clay (<0.002 mm). The source rock was mainly massive and little weathered. There was negligible soil, moraine, or talus to entrain. Thus, about 1×10^7 m^3 of fine materials were produced by the rock avalanches (8).

The deposits, classed as a diamicton, lacked linear and planar structures or sorting, but showed a crude inverse grading. Boulders increased toward the top and formed the surface layer. Large clasts were matrix-supported in most sections. Clast-supported boulders occurred in sections at the distal rim (Fig. 4).

The rocks maintained their relative stratigraphic position during movement to form bands of distinct color and texture in the deposits. The outer 100 to 300 m of each slide consisted of a fine-grained, light-gray, calcitic marble, which suggests that the original surfaces of failure and sliding were at the base of carbonate rocks. Other bands consisted of schist, quarzite, and dolomite marble.

Similar features have been reported for the surface of other rock avalanches, but their sedimentology in depth has rarely been observed. At the base of the Bualtar deposits, coarse clasts were of mixed rock type, and intermixing had occurred at the margins of bands. Otherwise, throughout each section, clasts larger than fine-sand size were distributed in homogeneous lithologic bands: carbonate clasts were only in carbonate bands, and schist clasts were only in schist bands. Finer materials departed slightly from this distribution, however.

On the one hand, the composition of fines is predominantly that of their lithological band. Major element analyses, with x-ray fluorescence, indicate that, in general, the fines have a similar composition to the surrounding coarse fraction. On the other hand, in all samples, the fines contained "exotic" minerals from other lithological bands. This distribution was first noticed in grain size analysis. Powdered talc occurred as fine material below 0.2 mm in diameter even where it was not present in the coarse material in the same band. Talc-rich schist, present in some narrow bands in the inner parts of the deposits, had diffused in powder form throughout. Tests for carbonate in fines showed 5 to 10% in bands with none or trivial amounts in the coarse materials. X-ray diffraction confirmed that powdered talc, calcite, and chlorite had diffused to all parts of the deposits (9). Analysis by size

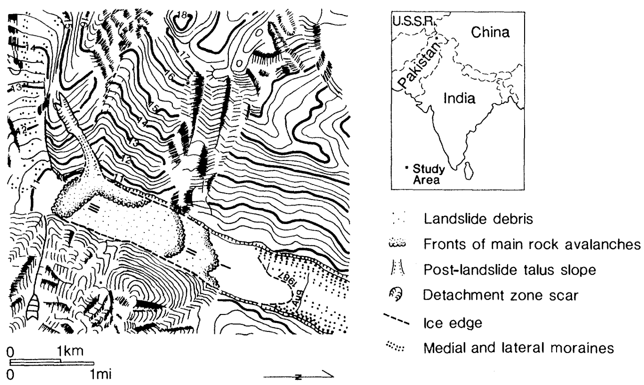

Fig. 1. Location of Bualtar Glacier, and map showing the extent of rock avalanche deposits on its surface in August 1986 and their frontal position in August 1987, after the glacier's sharp acceleration. Contours redrawn from (16), contour interval is 1000 feet; numbers along heavy contour lines are in 10,000 feet.

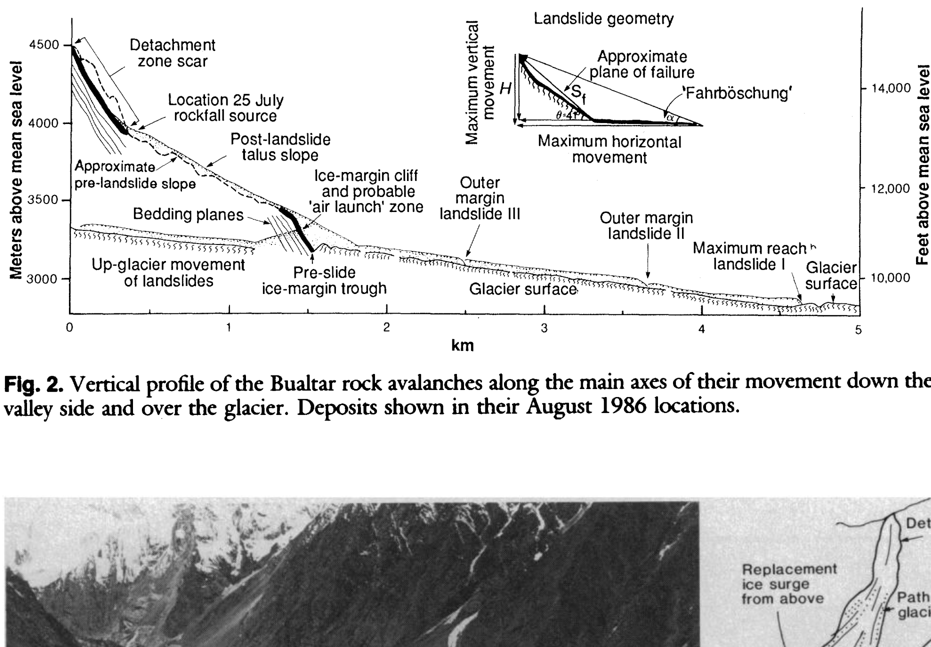

Fig. 2. Vertical profile of the Bualtar rock avalanches along the main axes of their movement down the valley side and over the glacier. Deposits shown in their August 1986 locations.

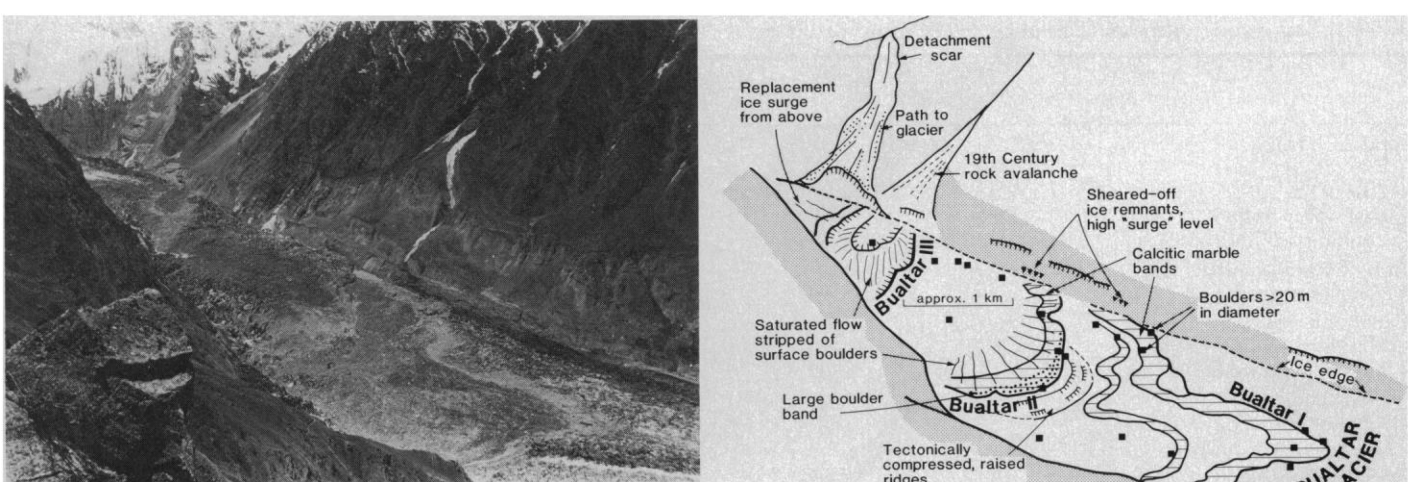

Fig. 3. (**Left**) View of the three Bualtar rock avalanche deposits. This photo was taken after the glacier surge. [Photo K. Hewitt, 25 May 1987] (**Right**) Important features in the photo.

fraction showed that only materials finer than intermediate sand dispersed through the mass during the landslide process. Coarser particles had not.

There were large amounts of powdered calcite. Most were produced by grinding and crushing, but a portion of the carbonate seemed to have been calcined by the landslide. Below the surface, the fines were distinctly caustic everywhere, but most noticeably in sections in marble bands in the distal part of the landslide. Here, after breaking up, the deposits resembled the waste heaps of lime kiln operations and caused some frothing in pools of water they slid into. I lost a layer of skin from my hands after each sampling episode, which is an indication of lime burn. On moraines and slopes within 0.5 km of the deposits, the ubiquitous mosses were killed off, presumably because the dustfall was also caustic (*10*).

Rock dissociation in carbonate landslides has been predicted but never observed (*11*). Voight and Faust have shown that temperatures sufficient to calcine limestone are possible in large rockslides and may cause large strength loss and acceleration (*12*). Sufficient frictional heating can occur only at the base of a rockslide once a critical velocity is attained, but before the rockslide reaches very high velocities or breaks up, when heat will diffuse too rapidly. Because the lime originates at the base of the sliding mass, it may be significant in the run-out zone too. Quicklime combines readily and often explosively with available moisture (whether vapor, liquid, or ice), which results in fine powder. Such a process may have assisted in the wide diffusion of powdered carbonate in the Bualtar slides. The heat of hydration after deposition, about 100 cal kg^{-1}, could help melt ice.

Naturally generated limes in large carbonate landslides may easily go unreported. Relative to total mass, the amounts of lime produced will be small because of the constraints noted above. The hydroxides recarbonate and weather rapidly in the presence of air and percolating moisture. How much calcination occurs may thus be impossible to determine empirically. Analytical techniques, developed for the lime industry, are for fresh and almost pure samples (*13*). Those from a rock avalanche are highly contaminated products that are subjected to massive pulverizing, diffusion, dilution, and weathering.

Given that a large fraction of all rock avalanches are in carbonates, calcination may have been important in other avalanches, as well. The production of a large amount of fine materials in the deposits has major implications for understanding the significance of rock avalanches for high-mountain erosion. This disaggregation has generally not been emphasized because of a focus upon processes that would reduce friction. The Bualtar deposits record tremendous grinding, fracturing, and comminution. Most of that occurred in descent to and impact with the glacier. However, there is much evidence that it continued in the run-out zone. For example, coarse clasts in regions with mixed lithologies have halos of pulverized fine material, threads of which extend from the halo into the surrounding, homogeneous matrix. One important observation is that all sizes of clasts were not abraded equally. Sand-sized materials were very angular (*14*), being typically sharp edged and blade shaped. Coarser particles in the same samples had rounded edges, were more compact, and were subangular and subrounded.

Fig. 4. View along the rim of the deposits in the central part of the glacier. Melting of adjacent ice and collapse of the debris have revealed the diamicton in cross section. [Photo K. Hewitt, 1 June 1987]

The features described seem at odds with those models of rock avalanches with little internal friction to explain mobility or with the mere transport of already pulverized material in the run-out zone (*15*). However, Bualtar I deposits are in accord with Hsü's notion of "a dispersal of blocks in a dust cloud" (*5*). Momentum is imparted by collision of coarser clasts that tend to migrate to the top, but not laterally. Interstitial dust, as well as heated gases, including vaporized water, will reduce the effective normal pressure, adding to mobility. Yet, crushing of smaller particles between colliding boulders and rounding of coarser materials can continue. These flow conditions allow finer materials to diffuse through and out of the rock avalanche.

Four other historic and prehistoric rock avalanche deposits were found in the same basin, reflecting a long history of avalanche activity. Their catastrophic nature and evidence of past occurrences make rock avalanches a serious geological hazard in the Karakoram.

Table 1. Bualtar rock avalanches: dimensions and estimated parameters (*16*).

	All	Bualtar I	Bualtar II	Bualtar III
Altitudinal range (m)*				
Top of scar	4450			
Base of scar	4250			
Base, valley wall	3230			
Lowest reach of deposits		2960	3020	3150
Area of debris on glacier (km^2)		4.1	3.3	1.2
Volume of deposits ($10^{6}\ ^{3}$)		10.0	7.0	3.0
Travel of debris				
Maximum vertical, H (m)		1490	1430	1300
Maximum horizontal, L (m)		4800	3700	2400
Fahrböschung, (α°)†		17°13′	20°48′	28°22′
Coefficient of friction,				
$\mu = (H/L) = \tan \alpha$		0.3	0.4	0.5
Excess travel (km)		2.4	1.5	0.3

*Meters above sea level. †The fahrböschung angle, coefficient of friction, and excess travel are defined in (*5*) and Fig. 2 (inset).

REFERENCES AND NOTES

1. "Rock avalanche" is widely used in North America for rockslides that generate catastrophic run-out of fragmented rock. "Rockfall-" and "rockslide-avalanche" are more fully descriptive but cumbersome.
2. The rock avalanche buried an array of stations used to monitor movement and ablation by our glacier hydrology program.
3. A. Desio, *Geological Tentative Map of the Western Karakoram* (Institute of Geology, Milano, 1964).
4. Temperature data show that freeze-thaw cycles con-

tinued at the altitudes where the rock avalanche originated. (K. Hewitt, unpublished data).
5. K. J. Hsü, *Geol. Soc. Am. Bull.* **86**, 129 (1975).
6. Average speed to the glacier is given by $v_m = 0.5at$, where $a = g(\sin\Theta - \mu\cos\Theta)$, the acceleration, and the time $t = \sqrt{2s/a}$. Θ is the average slope to the glacier (41°); the slope distance s = 1860 m, and the coefficient of friction μ = 0.31. Maximum velocity was estimated from: $v_{max} = \sqrt{2as}$. These elementary formulas give fair approximations to observed rock avalanche velocities. The equations are defined and discussed by K. J. Hsü [in B. Voight, Ed., *Rockslides and Avalanches* (Elsevier, Amsterdam, 1978), vol. 1, pp. 84–85]. Velocity estimate over the glacier is from: $v_r = \sqrt{2gh}$, where h is the height of rises it had to climb (100 m).
7. Typical features identified in M. R. Mudge [*Geol. Soc. Am. Bull.* **76**, 1003 (1985)] and G. H. Eisbacher [*Can. Geotech. J.* **16**, 309 (1979)].
8. Sampling was dependent on accessibility, but covered 40 locations. Analyses quoted in the report refer to 12 test samples from across Bualtar I. The later, saturated deposits are broadly similar.
9. Carbonate, by LECO carbon determinator, and x-ray fluorescence, courtesy Dr. R. H. McNutt, McMaster University, Ontario. X-ray diffraction courtesy Dr. L. Evans, Guelph University, Ontario.
10. Pointed out by Dr. J. S. Gardner (personal communication) during a visit in May 1987.
11. T. H. Erismann, *Rock Mech.* **12**, 15 (1979).
12. B. Voight and C. Faust, *Geotechnique* **32**, 43 (1982). See also H. Heuberger *et al.*, *Mt. Res. Develop.* **4**, 345 (1984); they describe fused rock or "frictionite" due to high temperatures at the base of two large Pleistocene landslides.
13. R. S. Boynton, *Chemistry and Technology of Lime and Limestone* (Wiley, New York, ed. 2, 1980).
14. M. Powers, *J. Sediment. Petrol.* **23**, 117 (1953).
15. R. L. Shreve, *Science* **154**, 1639 (1966); P. E. Kent, *J. Geol.* **74**, 79 (1968).
16. X. X. Shipton, *1939 Expedition Original Survey Sheets* (Royal Geographical Society, London, 1939).
17. I thank D. M. Cruden, S. G. Evans, D. K. Keefer, B. H. Luckman, and G. Subins for helpful reviews of the draft paper; M. Stone for laboratory assistance and P. Schaus for preparing figures. The Snow and Ice Hydrology Project is funded by The International Development Research Centre, Ottawa; Pakistan's Water and Power Development Authority, and Wilfrid Laurier University's Office of Research.

29 July 1988; accepted 9 August 1988

Regulation of a Heart Potassium Channel by Protein Kinase A and C

KENNETH B. WALSH AND ROBERT S. KASS

The enzymes adenosine 3′,5′-monophosphate (cAMP)–dependent protein kinase (protein kinase A) and protein kinase C regulate the activity of a diverse group of cellular proteins including membrane ion channel proteins. When protein kinase A was stimulated in cardiac ventricular myocytes with the membrane-soluble cAMP analog 8-chlorphenylthio cAMP (8-CPT cAMP), the amplitude of the delayed-rectifier potassium current (I_K) doubled when recorded at 32°C but was not affected at 22°C. In contrast, modulation of the calcium current (I_{Ca}) by 8-CPT cAMP was independent of temperature with similar increases in I_{Ca} occurring at both temperatures. Stimulation of protein kinase C by phorbol 12,13-dibutyrate also enhanced I_K in a temperature-dependent manner but failed to increase I_{Ca} at either temperature. Thus, cardiac delayed-rectifier potassium but not calcium channels are regulated by two distinct protein kinases in a similar temperature-dependent fashion.

PROTEIN KINASES MODULATE THE electrical activity of various cells through their actions on membrane ion channels (*1–3*). In cardiac muscle, enhancement of the voltage-gated L-type calcium current (I_{Ca}) by β-adrenergic agonists, such as isoproterenol, may result from a direct phosphorylation of Ca^{2+} channel protein by cAMP-dependent protein kinase (protein kinase A) (*4–6*). In smooth muscle and neuronal cells, another protein kinase (protein kinase C), activated by diacylglycerol (or synthetic phorbol ester compounds) and intracellular Ca^{2+} (*7*), regulates a number of K^+ and Ca^{2+} currents (*8–12*).

Isolated ventricular cells were obtained from adult guinea pig hearts by a procedure similar to that of Mitra and Morad (*13*). Recordings of membrane currents were made with the whole-cell patch clamp technique (*14*) in a chamber containing normal external solution consisting of 138 mM NaCl, 4.8 mM KCl, 1.2 mM $MgCl_2$, 1.0 mM $CaCl_2$, 5 mM dextrose, 5 mM Hepes, and 5 μM tetrodotoxin (TTX), pH 7.4. Electrodes (2 to 5 megohms) contained 50 mM KCl, 60 mM potassium glutamate, 2 mM $MgCl_2$, 1 mM $CaCl_2$, 11 mM EGTA, 5 mM adenosine triphosphate, and 10 mM Hepes. The ratio of EGTA to $CaCl_2$ sets the free intracellular Ca^{2+} concentration at 10 nM (*15*). The pH of this solution was adjusted to 7.3 with KOH, bringing the total K^+ concentration to 140 mM. The temperature of the recording chamber was set at either 22° or 32°C. In order to study I_{Ca} and I_K, cell membrane potential was held at −30 mV to inactivate the fast Na^+ current. The I_{Ca} was elicited by test pulses at 40-ms duration to potentials of −10 to +10 mV, and I_K deactivating tails were recorded on return to the holding potential after a 1.5-s prepulse to +20 through +40 mV. Protein kinase A and C were stimulated by external application of 8-CPT cAMP (Boehringer Mannheim) and phorbol 12,13-dibutyrate (PDB) (Sigma), respectively, to the recording chamber.

Addition of 150 μM 8-CPT cAMP to a cell at 22°C produced little change in the I_K tails but caused over a threefold increase in the amplitude of I_{Ca} (Fig. 1A and Table 1). The modulation of I_{Ca} provides evidence that exposure to 8-CPT cAMP stimulates protein kinase A in these cells. Enhancement of I_{Ca} by 8-CPT cAMP occurred in a voltage-dependent manner, with the largest change in I_{Ca} occurring at more negative potentials (Table 1). A similar voltage-dependent increase in I_{Ca} has been reported during stimulation of the β-receptor with isoproterenol (*16*).

At 32°C, I_K doubled in size in the presence of 8-CPT cAMP, whereas I_{Ca} was enhanced to an extent similar to that at 22°C (Fig. 1B and Table 1). As was the case with I_{Ca}, the enhancement of I_K mediated by protein kinase A occurred in a voltage-dependent manner. The increase in tempera-

Table 1. Summary of changes in amplitude of I_K and I_{Ca} during stimulation by protein kinase A and C. All values represent the mean ± SEM (n = 4 for all experiments except 8-CPT cAMP at 22°C, where n = 3). I_K tails were recorded on return to the holding potential (−30 mV) after a 1.5-s prepulse to the indicated potential.

Condition	I_{Ca} Potential (mV)	I_{Ca} Change in amplitude (%) at 22°C	I_{Ca} Change in amplitude (%) at 32°C	I_K Potential (mV)	I_K Change in amplitude (%) at 22°C	I_K Change in amplitude (%) at 32°C
150 μM 8-CPT cAMP	−10	549 ± 130	607 ± 156	20	16 ± 2	154 ± 21
	0	220 ± 55	237 ± 55	30	12 ± 6	124 ± 11
	10	111 ± 19	97 ± 33	40	3 ± 2	92 ± 16
	20	84 ± 10	80 ± 29			
10 nM PDB	−10	1 ± 16	7 ± 9	20	−2 ± 4	46 ± 4
	0	−10 ± 10	−6 ± 3	30	−3 ± 4	49 ± 5
	10	−9 ± 10	3 ± 6	40	−1 ± 4	45 ± 5
	20	−5 ± 3	9 ± 6			

Department of Physiology, University of Rochester, School of Medicine and Dentistry, Rochester, NY 14642.